Publishing Excellence
Inspiring Progress
ARISTON PUBLICATIONS
Quantum Advances
ISSN: 3143-0724 www.aristonpubs.com/journal/quantum-advances https://doi.org/10.69626/qa.2025.0034

RESEARCH ARTICLE

Influence of external electric field on second harmonic generation for oblate CdS / ZnSe / CdSe quantum dots

J. M. Lozano-Saldivar[1], K. A. Rodríguez-Magdaleno[2,3*], G. Rodríguez-Guijarro[4], J. C. Jiménez-Soriano[5], B. E. Maldonado-Villa[2], F. M. Nava-Maldonado[1], J. C. Martínez-Orozco[2]

ABSTRACT: This work presents a theoretical study of electronic energy levels and second harmonic generation (SHG) in core–shell–shell quantum dots (QDs). Specifically, II–VI semiconductor nanostructures of the CdS/ZnSe/CdSe system are investigated, with particular emphasis on oblate core–shell–shell quantum dots. The analysis is performed both in the absence and in the presence of an external electric field to evaluate its influence on the electronic and optical properties of the system. The electronic structure is modeled using the effective mass approximation (EMA), and the Schrödinger equation is solved via the finite difference method. The results reveal a strong dependence of energy levels and nonlinear optical response on geometric and structural composition. In particular, the SHG response is shown to be highly sensitive to both core size and external electric field, enabling controlled modulation of optical properties. These findings highlight the potential of engineered QDs for applications in optoelectronics and biophotonics, where SHG processes can enhance imaging resolution and sensitivity. Overall, this study provides valuable insight into the role of geometry and external fields in tailoring the properties of semiconductor nanostructures, with implications for future developments in nanotechnology, photonics, and quantum-based applications.

Keywords: Quntum dots; Second-harmonic generation; Semiconductor nanostructures; CdS/ZnSe/CdSe.

Received: 04 October 2025; Revised: 13 November 2025; Accepted: 25 November 2025; Published Online: 11 December 2025

1. INTRODUCTION

Since their discovery, quantum dots (QDs) have been extensively studied both theoretically and experimentally. Early investigations demonstrated that energy quantization in these systems strongly depends on their size, opening the possibility of designing materials with tunable properties [1] Consequently, the development of DQs represents one of the most significant advances in modern nanotechnology. The importance of these advances was recognized with the Nobel Prize in Chemistry in 2023 [2], awarded to Moungi G. Bawendi, Louis E. Brus, and Aleksey Yekimov for the discovery and synthesis of quantum dots, highlighting the impact of fundamental research on applied technologies.

Despite extensive research, challenges remain in understanding how structural parameters and external perturbations influence the optoelectronic behavior of quantum dots (QDs). Moreover, recent advances have made it possible to consider core–shell structures rather than only single-material QDs. In this context, spherical symmetry remains one of the most commonly employed approximations in modeling

[1] Unidad Académica de Ciencias Químicas, Universidad Autónoma de Zacatecas. Zac., Zacatecas, México.
[2] Unidad Académica de Física, Universidad Autónoma de Zacatecas. Zac., Zacatecas, México.
[3] Laboratorio de Ciencias Forenses, Unidad Academica de Derecho, Universidad Autónoma de Zacatecas Zac., Zacatecas, México.
[4] Department of Physics, University of North Texas, Denton, TX, USA.
[5] Unidad Académica de Estudios Nucleares, Universidad Autónoma de Zacatecas, Zac., Zacatecas, Mexico.

* Author to whom correspondence should be addressed: karelyrod@uaz.edu.mx (K. A. Rodríguez-Magdaleno)

© Ariston Publications 2025. All rights reserved.

core–shell and multi-shell quantum dots, owing to its mathematical simplicity and the possibility of obtaining analytical solutions [3, 4]. A wide range of materials has been explored in core–shell nanostructures, including III–V systems such as InP/ZnSe/ZnS and GaAs/AlGaAs, as well as II–VI compounds such as CdSe/ZnS and ZnTe/ZnSe/ZnS [5]. Nevertheless, increasing attention has been devoted to more complex geometries, which introduce anisotropy and additional confinement effects, offering flexibility for tuning electronic and optical properties [6, 7].

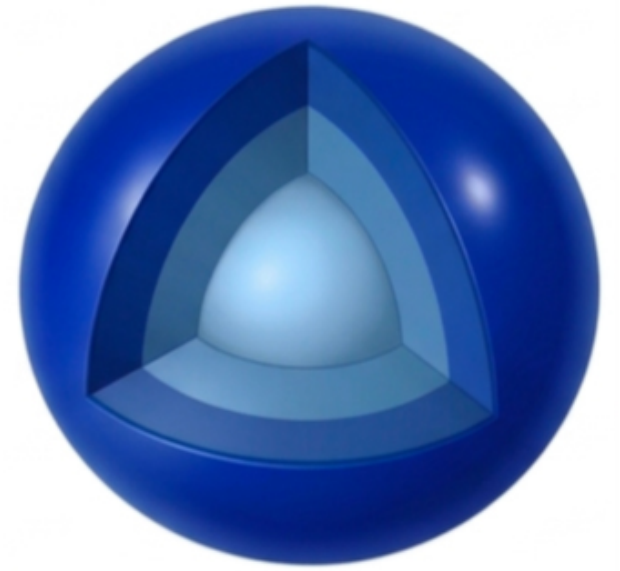


Fig. 1. Schematic representation of a core–shell–shell quantum dot.

In particular, II–VI semiconductor systems such as CdSe, ZnSe, and CdS exhibit high chemical stability and luminescence efficiency, making them suitable for optoelectronic and biomedical applications, after bio-functionalization. The combination of these materials in multilayered nanostructures enables reduced nonradiative recombination and improved control over electronic and optical properties. However, several effects—particularly structural strain and its interplay with external fields and non-spherical geometries—remain insufficiently explored. In this context, the present study focuses on a detailed theoretical analysis of second harmonic generation, incorporating external electric fields and an oblate ellipsoidal geometry to provide a more comprehensive understanding of these systems [5, 8]. When a core–shell–shell structure is formed, lattice mismatch between the different materials induces strain at the interfaces, which alters the electronic structure through deformation potentials. In multilayered systems, strain distributions become increasingly complex, requiring continuum elasticity theory for accurate modeling [9, 10].

Nonlinear optical phenomena—such as second and third harmonic generation (SHG and THG)—have attracted considerable attention in II–VI semiconductor quantum dots due to their strong dependence on quantum confinement [11–13]. For example, Mantashian et al. [14] showed that decreasing the dot radius leads to a blue shift in absorption, while larger structures exhibit enhanced nonlinear contributions and increased SHG and THG intensities accompanied by a red shift, highlighting the critical role of size and confinement in nonlinear optical behavior. Their relevance is further supported by applications in bioimaging and biological labeling, where sensitivity to environmental and structural conditions enables high-resolution and selective probing [15, 16]. Recent studies have also examined the influence of dielectric environment, structural parameters, impurities, and external electric fields on nonlinear optical responses in CdSe/ZnS-based systems [17]. Similarly, Karakoc et al. [18] demonstrated that both geometric parameters and the surrounding dielectric medium significantly affect energy levels, dipole matrix elements, and SHG/THG responses in ZnS/CdSe quantum dots.

The paper is organized as follows. Section 2 presents the theoretical framework. Section 3 provides the results and discussion. Section 4 summarizes the main conclusions. Finally, the acknowledgements and references are given. .

2. THEORETICAL FRAMEWORK

The methodological foundations required for the theoretical study of QDs are presented, aiming to accurately predict and determine their electronic properties, as well as second harmonic generation. In this context, one of the most widely used theoretical frameworks for studying semiconductor nanostructures is the effective mass approximation within the envelope function approximation (EFA), with equation:

$$-\frac{\hbar^2}{2m^*}\nabla^2\Psi(\vec{r}) - e\,\vec{F}\cdot\vec{r} + V(\vec{r})\,\Psi(\vec{r}) = E\,\Psi(\vec{r}) \quad (1)$$

where $\hbar$ is the reduced Planck constant, m^* is the effective mass of the electron in the material, $\Psi(\vec{r})$ is the envelope function, e is the electron charge, $\vec{F}$ is the applied external electric field, and $V(\vec{r})$ is the confinement potential.

Due to the system's symmetry and axial symmetry

 © Ariston Publications 2025. All rights reserved.

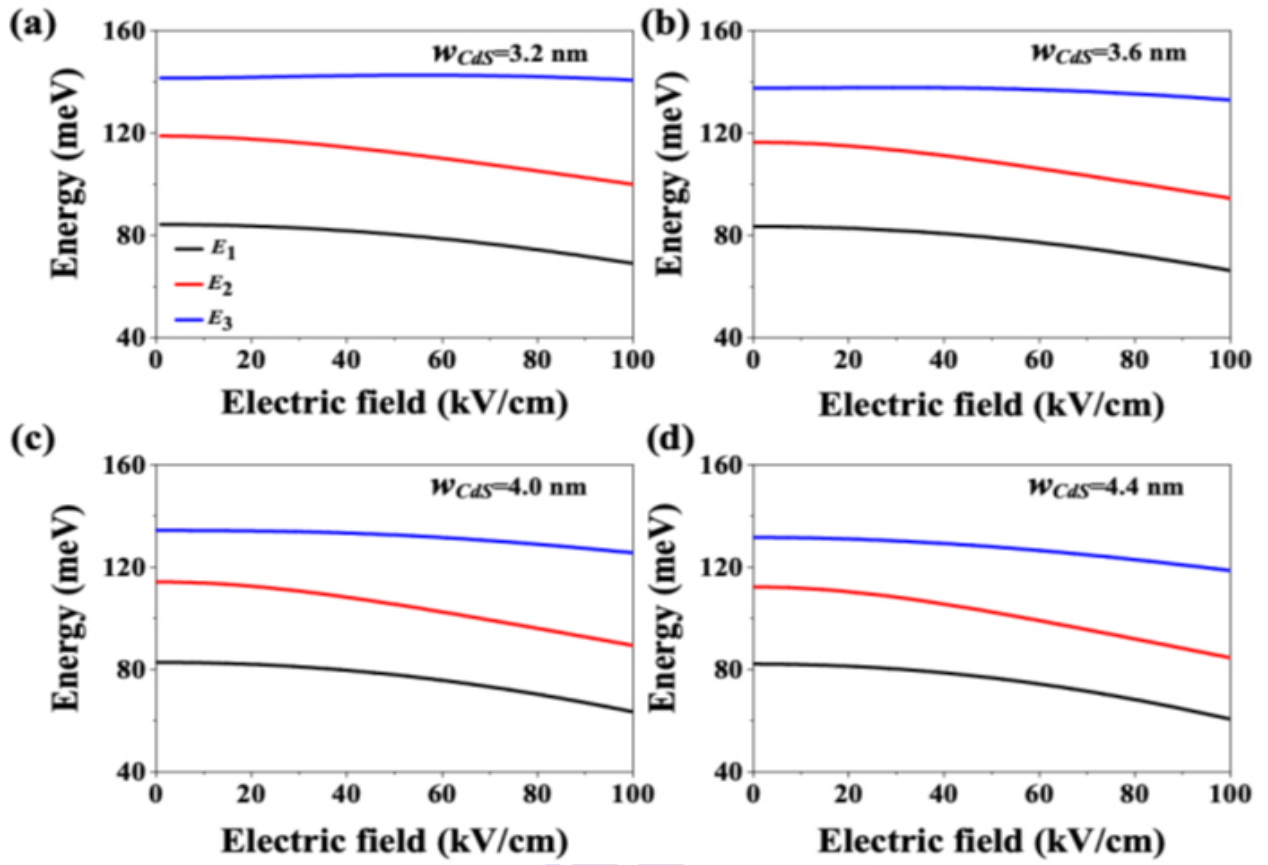


Fig. 2. Energy levels of an oblate ellipsoidal CdS/ZnSe/CdSe QD as a function of the electric field for different CdS core widths $w_CdS(nm)$: $(a)3.2, (b)3.6, (c)4.0, and (d)4.4nm, with fixed shell widths of w_{ZnSe}$ = 0.99 nm and w_{CdSe} = 3.6 nm.

with respect to the z-axis, we can work in cylindrical coordinates, $\vec{r} = (\rho, \phi, z)$. Thus, the envelope function can be expressed as $\Psi(\rho, \phi, z) = \Phi(\rho, z) = e^{im_l\phi}$, where $m_l = 0, \pm1, \pm2, \ldots$ is the angular momentum quantum number. The equation that determines $\Phi(\rho, z)$ is given by:

$$-\frac{\hbar^2}{2m^*}\left[\frac{\partial^2}{\partial\rho^2}+\frac{1}{\rho}\frac{\partial}{\partial\rho}+\frac{\partial^2}{\partial z^2}-\frac{m_l^2}{\rho^2}\right]\Phi(\rho,z) + [eFz + V(\rho,z)]\,\Phi(\rho,z) = E\,\Phi(\rho,z) \tag{2}$$

with the electric field applied along the z-axis, where the potential profile $V(\rho, z)$ is given by:

$$V(\rho,z) = \begin{cases} V_{\text{CdS}}, & 0 \le r \le \rho_1 \\ V_{\text{ZnSe}}, & \rho_1 < r \le \rho_2 \\ 0, & \rho_2 < r \le \rho_3 \\ \infty, & r > \rho_3 \end{cases} \tag{3}$$

where $V_{\text{CdS}} = E_c^{\text{CdS}} - E_c^{\text{CdSe}}$ and $V_{\text{ZnSe}} = E_c^{\text{ZnSe}} - E_c^{\text{CdS}}$, with:

$$E_c = E_c^0 + a_c\frac{\Delta\Omega}{\Omega} \tag{4}$$

When analyzing CdS/ZnSe/CdSe core-shell-shell quantum dots, it is essential to consider the effects of mechanical strain arising from lattice mismatch between the semiconductor materials that constitute the nanostructure. This mismatch induces deformations in the crystal lattice, which significantly modify the electronic structure and, consequently, the optical properties of the system. The theoretical description of these effects is based on the formalism developed by Tudor E. Pahomi et al. [10], in which the strain distribution and its impact on the potential profiles and effective parameters of the system are modeled. This approach allows for the consistent incorporation of deformation effects into the electronic structure and leads to the numerical evaluation of Eq. 4. All the relevant parameters are reported in Table 1.

© Ariston Publications 2025. All rights reserved.

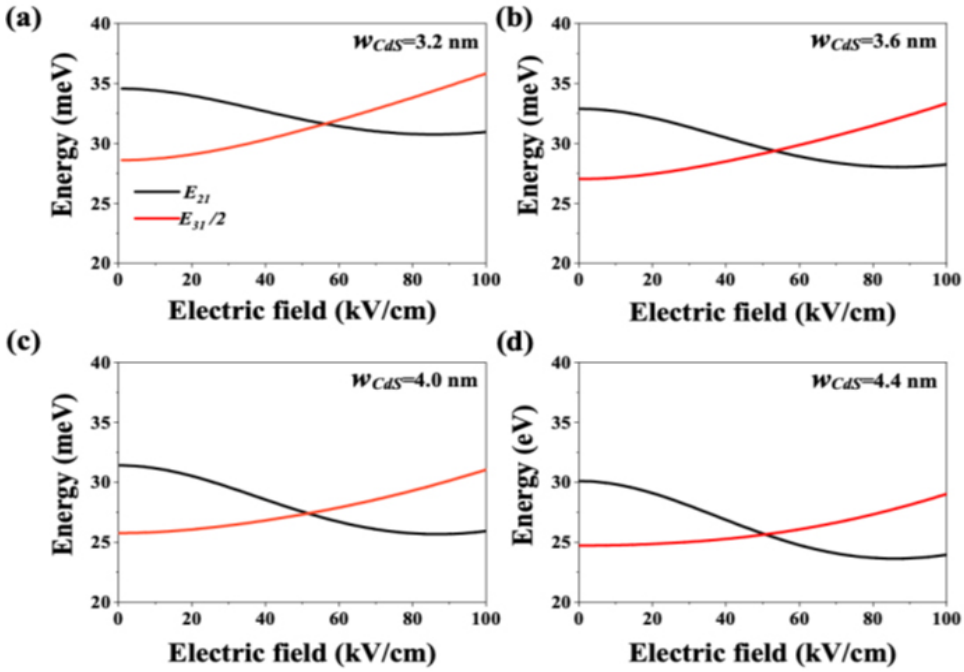


Fig. 3. Energy levels differences of an oblate ellipsoidal CdS/ZnSe/CdSe QD as a function of the electric field for different CdS core widths w_{CdS}(nm): (a) 3.2, (b) 3.6, (c) 4.0, and (d) 4.4 nm, with fixed shell widths of w_{ZnSe} = 0.99 nm and w_{CdSe} = 3.6 nm.

Table 1. Material's and Physical Parameters [9, 10]

Parameter	CdS	ZnSe	CdSe
$m^*(m_e)$	0.22	0.21	0.15
a (nm)	0.582	0.565	0.605
ν	0.410	0.376	0.408
E_g^0 (eV)	2.49	2.69	1.74
a_c (eV)	0.4	1.65	0.9
a_v (eV)	-2.54	-4.17	-2
E_v^0 (eV)	-6.42	-6.07	-6.00
σ_v (10^{24} m^{-3})		5.0	
τ (10^{-12} s)		2.0	

On the other hand, within the compact density matrix approach [19][19], the expression for third harmonic generation (SHG) is given by:

$$\chi_{2\omega}^{(2)}(\omega) = \frac{e^3\sigma_v}{\varepsilon_0} \times \frac{M_{12}M_{23}M_{31}}{(\hbar\omega - \Delta E_{21} + i\hbar\Gamma)} \times \frac{1}{(2\hbar\omega - \Delta E_{31} + i\hbar\Gamma)} \quad (5)$$

where ε_0 is the vacuum permittivity, σ_v is the charge density, ω is the angular frequency of the incident photon, and $\hbar\Gamma$ is the damping term associated with the transition lifetime. The energy differences are defined as $E_{ji} = |E_j - E_i|$. The product $M_{12}M_{23}M_{31}$ corresponds to the matrix elements M_{ij} associated with transitions between the i-th and j-th states.

3. RESULTS AND DISCUSSIONS

Here, we present the results for the electronic structure, dipole matrix elements, and second harmonic generation for the oblate ellipsoidal configuration of core–shell–shell quantum dots, as depicted in Figure 1, as functions of the applied electric field and geometric parameters. Unlike spherical geometry, this configuration exhibits spatial anisotropy, which significantly influences the electronic structure and optical properties of the system, enabling analysis of how geometric compression modifies the spatial distribution of electronic wave functions and the separation between energy levels.

Figure 2 shows the energy levels of an oblate ellipsoidal CdS/ZnSe/CdSe core-shell-shell quantum dot as a function of the applied electric field intensity. The variation of the first three conduction band states, E_1, E_2, and E_3, is presented, corresponding to the ground, first excited, and second excited states, respectively. Figures 2 (a)-(d) illustrate different CdS

 © Ariston Publications 2025. All rights reserved.

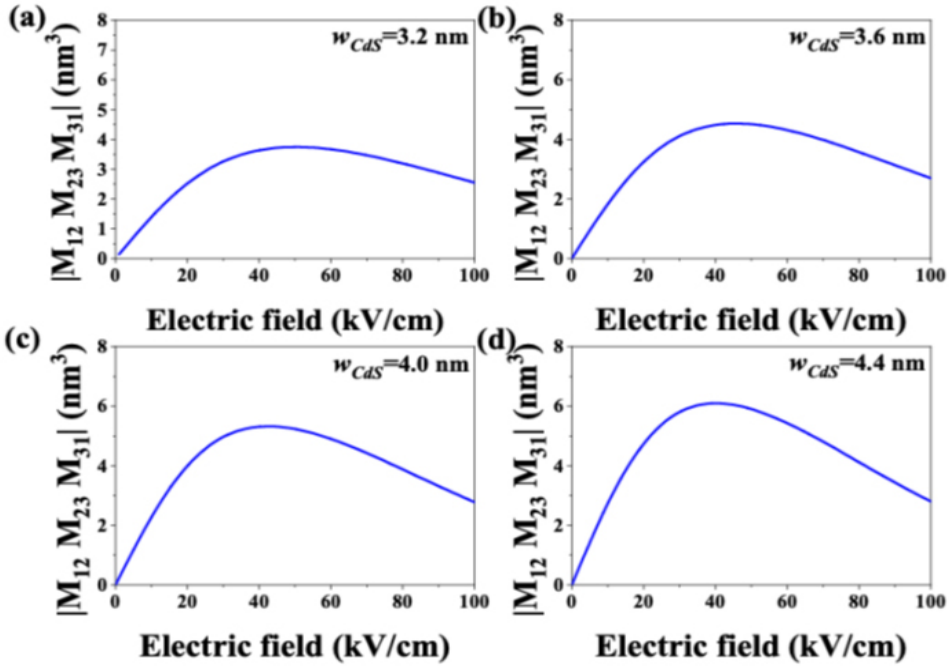


Fig. 4. Product of the matrix elements an oblate ellipsoidal CdS/ZnSe/CdSe QD as a function of the electric field for different CdS core widths w_{CdS} (nm): (a) 3.2, (b) 3.6, (c) 4.0, and (d) 4.4 nm, with fixed shell widths of w_{ZnSe} = 0.99 nm and w_{CdSe} = 3.6 nm.

core widths: (a) $w_{\mathrm{CdS}} = 3.2$ nm, (b) $w_{\mathrm{CdS}} = 3.6$ nm, (c) $w_{\mathrm{CdS}} = 4.0$ nm, and (d) $w_{\mathrm{CdS}} = 4.4$ nm, with fixed shell thicknesses of $w_{\mathrm{ZnSe}} = 0.99$ nm and $w_{\mathrm{CdSe}} = 3.6$ nm. As the electric field increases, all energy levels decrease. Additionally, increasing the core width results in slightly lower energy levels for a given field, due to reduced quantum confinement and the greater spatial extension of the electronic wave function.

Figure 3 shows the variation of the energy differences E_{12} and $E_{31}/2$ for an oblate ellipsoidal CdS/ZnSe/CdSe core--shell-shell quantum dot, using the same set of parameters reported in Figure 2. In all cases, the energy difference E_{12} (blue line) initially decreases with increasing electric field, reaches a minimum at intermediate values, and then increases at higher fields. In contrast, $E_{31}/2$ (orange line) increases almost monotonically with the electric field. A crossing between the two curves occurs at low field values, indicating the electric field range at which the double-resonant condition is achieved. This crossing shifts slightly with core width, appearing approximately between 45 and 50 kV/cm.

The variation of the product of the matrix elements $M_{12}M_{23}M_{31}$ for an oblate ellipsoidal CdS/ZnSe/CdSe core-shell-shell QD as a function of the applied electric field intensity is presented in Figure 4. This quantity is directly related to the transition probabilities between the first three electronic levels and is relevant for the analysis of nonlinear optical properties. Figure 4 (a)-(d) correspond to different CdS core widths: (a) $w_{\mathrm{CdS}} = 3.2$ nm, (b) $w_{\mathrm{CdS}} = 3.6$ nm, (c) $w_{\mathrm{CdS}} = 4.0$ nm, and (d) $w_{\mathrm{CdS}} = 4.4$ nm, with fixed outer layer thicknesses of $w_{\mathrm{ZnSe}} = 0.99$ nm and $w_{\mathrm{CdSe}} = 3.6$ nm. In all cases, the product increases rapidly at low electric field values, reaches a maximum around $E \approx 40$--50 kV/cm, and then decreases as the field increases further. This maximum coincides with the region near the crossing of electronic levels observed in Figure 3, where the energetic proximity of the states enhances their coupling and increases the overlap of the wave functions, thereby maximizing the transition probabilities. This behavior reflects the existence of an optimal condition in which the balance between quantum confinement and coupling between electronic states enhances the nonlinear response. For smaller values of w_{CdS}, strong confinement limits the overlap of the wave functions, reducing the magnitude of the matrix elements, whereas for larger values, reduced confinement leads to lower efficiency in resonant transitions. This parameter range allows us to present the SHG optical response as shown in Figure 4.

Figure 5 shows the second harmonic generation for the oblate configuration in the ellipsoidal geometry of a CdS/ZnSe/CdSe core--shell--shell quantum dot as a function of the incident photon energy and the applied electric field strength. Well-defined resonant

© Ariston Publications 2025. All rights reserved.

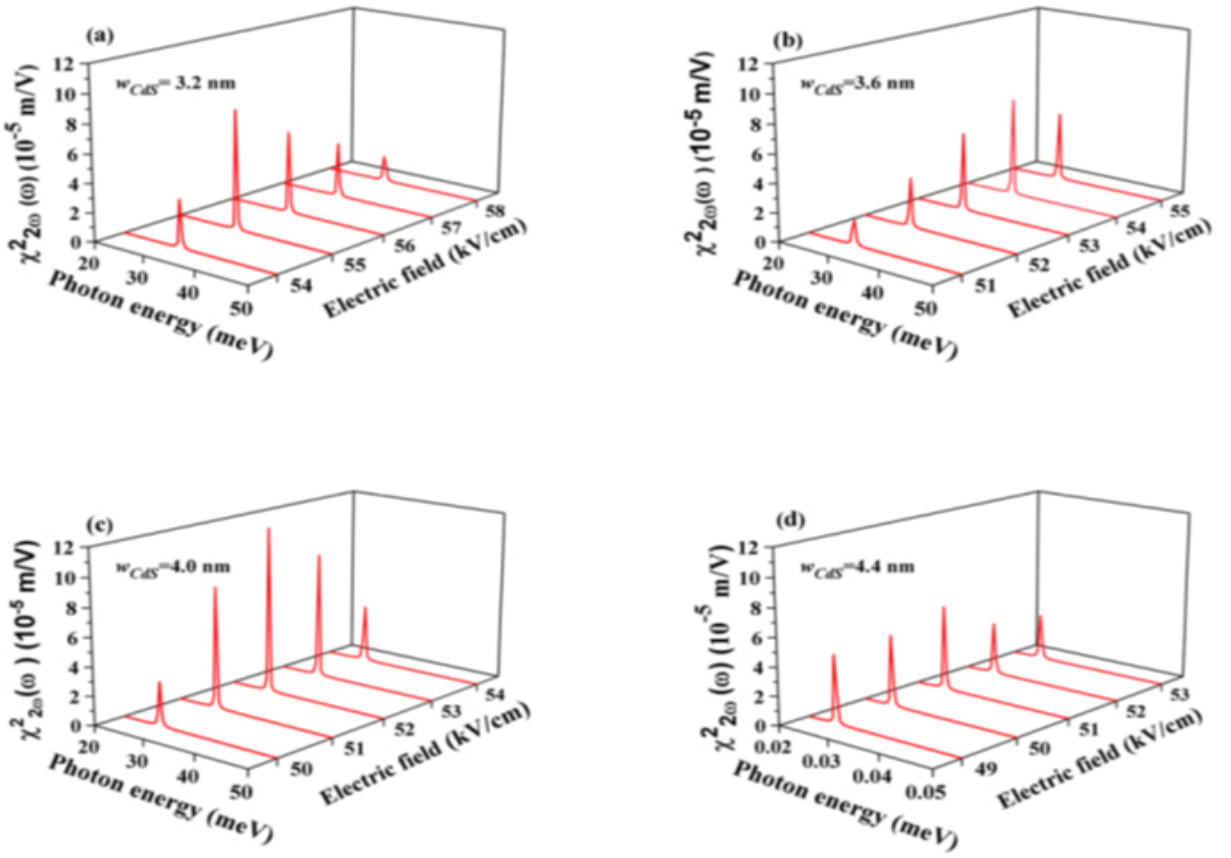


Fig. 5. Product of the matrix elements an oblate ellipsoidal CdS/ZnSe/CdSe QD as a function of the electric field for different CdS core widths w_{CdS} (nm): (a) 3.2, (b) 3.6, (c) 4.0, and (d) 4.4 nm, with fixed shell widths of w_{ZnSe} = 0.99 nm and w_{CdSe} = 3.6 nm.

peaks are observed for different CdS core widths w_{CdS}: (a) 3.2 nm, (b) 3.6 nm, (c) 4.0 nm, and (d) 4.4 nm, while the inner and outer shell thicknesses are fixed at $w_{\mathrm{ZnSe}} = 0.99$ nm and $w_{\mathrm{CdSe}} = 3.6$ nm. These peaks are associated with electronic transitions that satisfy the double-resonance condition, which coincides with the level crossing reported in Figure 3. A strong dependence of both the position and intensity of the peaks on the electric field is observed, as the field modifies the energy level structure and the wave functions of the system. As the electric field increases, the peaks shift in energy and vary in amplitude, indicating a significant modulation of the nonlinear response. The SHG reaches its maximum intensity of approximately 10^{-5} m/V for $w_{\mathrm{CdS}} = 4.0$ nm at an incident photon energy of about 27 meV and $F \approx 52$ kV/cm, indicating an optimal geometrical configuration for enhancing the nonlinear response. Furthermore, for all considered core sizes, the electric field corresponding to the maximum response remains within a narrow range of approximately 49--58 kV/cm. This suggests that the condition for maximum SHG is largely independent of the core size within the studied range.

4. CONCLUSION

In conclusion, this work analyzes the effects of CdS core size and an externally applied electric field on the electronic structure and transition properties of oblate CdS/ZnSe/CdSe core–shell–shell quantum dots. The results show that both geometry and core size play a key role in modulating quantum confinement and the resulting energy level distribution. The application of an external electric field provides effective control over transition energies and matrix elements, leading to significant modifications in the system. In particular, the occurrence of level crossings and the emergence of maxima in the matrix element products highlight the strong interplay between the electronic structure and the nonlinear optical response. The SHG within this energy range is especially relevant in biotechnology due to its ability to interact with characteristic vibrational modes of biomolecules. In this context, second harmonic generation in quantum dots emerges as a promising tool for converting these signals into spectral regions that are easier to detect, opening new possibilities forimaging, the development of

 © Ariston Publications 2025. All rights reserved.

advanced imaging, sensing, and biomedical diagnostic techniques characterized by high selectivity and non-invasive operation.

DECLARATIONS

Ethical Approval

We affirm that this manuscript is an original work, has not been previously published, and is not currently under consideration for publication in any other journal or conference proceedings. All authors have reviewed and approved the manuscript, and the order of authorship has been mutually agreed upon.

Funding

K. A. Rodríguez-Magdaleno acknowledges the financial support through project CBF-2025-I-3459, entitled "Desde el confinamiento cuántico a la funcionalidad: estudio de las propiedades eléctricas y ópticas de nanoestructuras y sus aplicaciones", a project supported by SECIHTI in 2025.

Availability of data and material

All of the data obtained or analyzed during this study is included in the report that was submitted.

Conflicts of Interest

The authors declare that they have no financial or personal interests that could have influenced the research and findings presented in this paper. The authors alone are responsible for the content and writing of this article.

Authors' contributions

J. M. Lozano-Saldivar: Writing original draft, Visualization, Software; K.A. Rodríguez-Magdaleno: Software, Investigation, Data curation, Conceptualization; G. Rodríguez-Guijarro: Software, Investigation, Data curation; J.C. Jiménez-Soriano: Investigation, Data curation; B.E. Maldonado-Villa: Software, Investigation, Data curation; F.M. Nava-Maldonado: Investigation, Data curation; J.C. Martínez-Orozco: Reviewing original draft, Data curation, Conceptualization.

REFERENCES

[1] Ekimov, A. I. and Onushchenko, A. A., **1981**. Quantum size effect in three-dimensional microscopic semiconductor crystals. *JETP Letters*, 34(6), p.345-349.

[2] Nobel Prize Outreach AB, **2023**. The Nobel Prize in Chemistry 2023, 10. NobelPrize.org. *Nobel Prize*.

[3] Tas, Hatice and Sahin, Mehmet, **2012**. The inter-sublevel optical properties of a spherical quantum dot-quantum well with and without a donor impurity. *Journal of Applied Physics*, 112, p.053717. https://doi.org/10.1063/1.4752461.

[4] Ebrahimipour, Bahareh Alsadat and Askari, Hassan Ranjbar and Ramezani, Ali Behjat, **2016**. Investigation of linear optical absorption coefficients in core-shell quantum dot (QD) luminescent solar concentrators (LSCs). *Superlattices and Microstructures*, 97, p.495. https://doi.org/10.1016/j.spmi.2016.06.017.

[5] Sahu, Anupam and Kumar, Dharmendra, **2022**. Core-shell quantum dots: A review on classification, materials, application, and theoretical modeling. *Journal of Alloys and Compounds*, 924, p.166508. https://doi.org/10.1016/j.jallcom.2022.166508.

[6] Shi, L. and Yan, Z. W., **2017**. Linear and nonlinear optical properties of an off-center donor in GaAs/AlGaAs and AlGaAs/GaAs core-shell ellipsoidal quantum dots. *Superlattices and Microstructures*, 109, p.382. https://doi.org/10.1016/j.spmi.2017.06.019.

[7] Osorio, J. A. and Caicedo-Paredes, D. and Vinasco, J. A. and Morales, A. L. and Radu, A. and Restrepo, R. L. and Martínez-Orozco, J. C. and Tiutiunnyk, A. and Laroze, D. and Hieu, Nguyen N. and Phuc, Huynh V. and Mora-Ramos, M. E. and Duque, C. A., **2020**. Pyramidal core-shell quantum dot under applied electric and magnetic fields. *Scientific Reports*, 10, p.8961. https://doi.org/10.1038/s41598-020-65442-x.

[8] Boyd, Robert W., **2020**. Nonlinear Optics. *Academic Press*.

[9] Van de Walle, Chris G., **1989**. Band lineups and deformation potentials in the model-solid theory. *Physical Review B*, 39, p.1871. https://doi.org/10.1103/PhysRevB.39.1871.

[10] Pahomi, Tudor E. and Cheche, Tiberius O., **2014**. Strain influence on optical absorption of giant semiconductor colloidal quantum dots. *Chemical Physics Letters*, 612, p.33. https://doi.org/10.1016/j.cplett.2014.08.021.

© Ariston Publications 2025. All rights reserved.

[11] Rahul, K. Suseel and Devaraj, Nayana and Babu, Rosmy K. and Mathew, Smitha and Salini, K. and Mathew, Vincet, **2017**. Intraband absorption of D- center in CdSe/CdS/CdSe/CdS multilayer quantum dot. *Journal of Physics and Chemistry of Solids*, 106, p.99. https://doi.org/10.1016/j.jpcs.2017.03.013.

[12] Chafai, A. and Essaoudi, I. and Ainane, A. and Ahuja, R., **2019**. Linear and nonlinear optical properties of donors inside a CdSe/ZnTe core/shell nanodot: Role of size modulation. *Results in Physics*, 14, p.102414. https://doi.org/10.1016/j.rinp.2019.102414.

[13] Cherni, A. and Yahyaoui, N. and Zeiri, N. and Said, M. and Saadaoui, S., **2023**. Simultaneous effect of the capped matrix and the geometric factors of CdS/ZnSe spheroidal quantum dots on the linear and nonlinear optical properties. *Optical and Quantum Electronics*, 55, p.273. https://doi.org/10.1007/s11082-023-04545-x.

[14] Mantashian, Grigor A. and Zaqaryan, Nare A. and Mantashyan, Paytsar A. and Sarkisyan, Hayk A. and Baskoutas, Sotirios and Hayrapetyan, David B., **2021**. Linear and Nonlinear Optical Absorption of CdSe/CdS Core/Shell Quantum Dots in the Presence of Donor Impurity. *Atoms*, 9, p.75. https://doi.org/10.3390/atoms9040075.

[15] Cox, Guy, **2011**. Biological applications of second harmonic imaging. *Biophysical Reviews*, 3, p.131. https://doi.org/10.1007/s12551-011-0052-9.

[16] Aghigh, Arash and Bancelin, Stephane and Rivard, Maxime and Pinsard, Maxime and Ibrahim, Heide and Legare, Francois, **2023**. Second harmonic generation microscopy: a powerful tool for bioimaging. *Biophysical Reviews*, 15, p.43. https://doi.org/10.1007/s12551-022-01041-6.

[17] Amin, N. and John Peter, A., **2024**. Role of surrounding dielectric matrices on the nonlinear properties of group II-VI core/shell dot in the presence of electric field. *Micro and Nanostructures*, 185, p.207728. https://doi.org/10.1016/j.micrna.2023.207728.

[18] Karakoc, M. and Naifar, A. and Bayrak, O., **2025**. Unveiling the impact of neighboring oxides: A detailed analysis of second and third harmonic generation in cylindrical ZnS/CdSe core/shell quantum dots. *Physica B*, 701, p.416961. https://doi.org/10.1016/j.physb.2025.416961.

[19] Sayrac, M. and Martínez-Orozco, J. C. and Mora-Ramos, M. E. and Ungan, F., **2022**. The nonlinear optical rectification, second and third harmonic generation coefficients of Konwent potential quantum wells. *European Physical Journal Plus*, 137, p.1033. https://doi.org/10.1140/epjp/s13360-022-03207-3.

ARISTON PUBLICATIONS

 © Ariston Publications 2025. All rights reserved.